ACS Photonics

Article

pubs.acs.org/journal/apchd5

Quasi-guiding Modes in Microfibers on a High Refractive Index Substrate

Kaiyang Wang,[†] Zhiyuan Gu,[†] Wenzhao Sun,[†] Jiankai Li,[†] Shumin Xiao,[‡] and Qinghai Song*[,†,§]

[†]Integrated Nanoscience Lab, Department of Electrical and Information Engineering, and [‡]Integrated Nanoscience Lab, Department of Material Science and Engineering, Harbin Institute of Technology, Shenzhen, China, 518055

[§]State Key Laboratory on Tunable Laser Technology, Harbin Institute of Technology, Harbin, China, 158001

ABSTRACT: Light confinement and amplification in micro- and nanofibers have been intensively studied, and a number of applications have been developed. However, typical micro- and nanofibers are usually free-standing or positioned on a substrate with lower refractive index to ensure the light confinement and guiding mode. Here we numerically and experimentally demonstrate the possibility of confining light within a microfiber on a high refractive index substrate. In contrast to the strong leakage to the substrate, we found that the radiation loss was dependent on the radius of the microfiber and the refractive index contrast. Consequently, quasi-guiding modes could be formed and the light could propagate and be amplified in such systems. By fabricating a tapered silica fiber and dye-doped polymer fiber and placing them on sapphire substrates, the light propagation, amplification, and consequent laser behaviors have been experimentally studied to verify the quasi-guiding modes in a microfiber on a higher index substrate. We believe that our research will be essential for the applications of microfibers and on-chip photonic circuits.

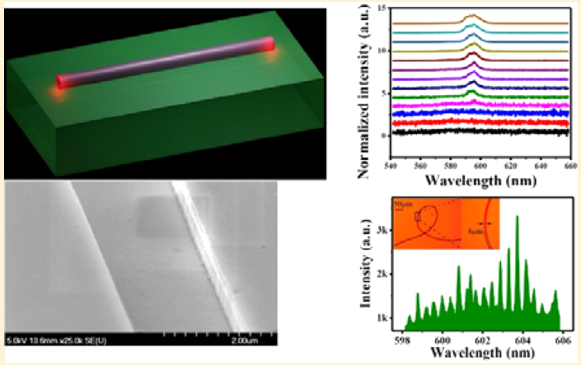

KEYWORDS: *quasi-guiding mode, microfiber, mask-free photolithography, knot cavity, light confinement and amplification*

With the rapid developments in nanoscience and nanotechnology, there is a strong demand for interconnection between on-chip micro- and nanocircuits and conventional optical elements. Compared with the conventional devices, microfibers (or nanofibers) have an extremely long distance in one dimension and well-defined microstructures (or nanostructures) in the other two dimensions.[1] Combined with their intrinsic advantages of low cost, easy fabrication, mechanical flexibility, and compatible integration with typical fiber systems, microfibers thus have been intensively studied as an effective bridge between typical optical elements (such as free space light source) and micro- and nanophotonic circuits. In the past few years, the applications of microfiber (nanofiber) have been further extended to optical couplers,[2,3] filters,[4,5] sensors,[6−8] nanolaser sources,[9−11] etc. Typically, the microfiber (nanofiber) is free-standing in air or on low refractive index solutions. Consequently, the diameter of a microfiber can be significantly reduced to as small as a few nanometers, and the interaction between the fiber and the environment has been dramatically improved. However, free-standing micro- and nanofibers have fatal disadvantages. They are extremely sensitive to environmental vibrations, making the devices very unstable.[12] For on-chip devices, the side to side coupling is much easier and more efficient than the end-fire injection.[13] However, this kind of coupling requires the light to propagate a short distance when the fiber is attached onto the substrate.

Several techniques have been developed to improve the stability of the fiber coupling system and light propagation on the substrate.[14−16] To ensure the light confinement within the microfiber, the refractive index contrast between fiber and substrate has been considered to be a key factor. Experimentally, micro- and nanosized silica fibers have been fixed on a MgF_2 substrate or an aerogel, which have very low refractive indices. For some applications on glass substrates, the refractive index of a fiber can also be increased to 2.08 by replacing silica with tellurite[17] or doping. Light can be well confined within micro- and nanofibers on these substrates. However, the materials of fibers and substrates are strongly restricted. For example, in practical applications, the substrates usually have higher refractive indices (e.g., Si, $n \approx 3.5$), which makes it extremely difficult to fabricate microfibers with an even higher refractive index. Very recently, slot waveguides and quasi-waveguides have also been proposed to confine light by applying low refractive index materials.[18,19] However, the former one is limited in nanostructure, whereas the latter one still confines light within the waveguides with higher effective refractive indices. Both of them are not directly compatible with conventional fiber systems. Therefore, it is very interesting and important to explore the possibility of confining and guiding

Received: April 6, 2015
Published: July 22, 2015

DOI: 10.1021/acsphotonics.5b00176
ACS Photonics 2015, 2, 1278−1283

light in low refractive index microfibers on a higher index substrate.

RESULTS AND DISCUSSIONS

Theoretical Analysis and Numerical Calculations. In a simple three-layer slab waveguide, the modes are the solutions of Maxwell's wave equation

$$\nabla^2\mathbf{E}(\mathbf{r}, t) = \frac{\left[\frac{n^2(r)}{c^2}\right]\partial^2\mathbf{E}(\mathbf{r}, t)}{\partial t^2} \quad (1)$$

where $\mathbf{E}$ is the electric field vector, $\mathbf{r}$ is the radius vector, $n(\mathbf{r})$ is the index of refraction, and c is the speed of light in a vacuum. For monochromatic plane waves, the modes can be calculated by introducing the boundary conditions. Equation 1 simply shows that modes cannot be formed in the region with a lower refractive index, which can be further confirmed by a numerical calculation. Two types of numerical methods that are based on the finite difference time domain (FDTD) method and finite element method (FEM) have been applied, and consistent results have been obtained. One result is shown in Figure 1a,

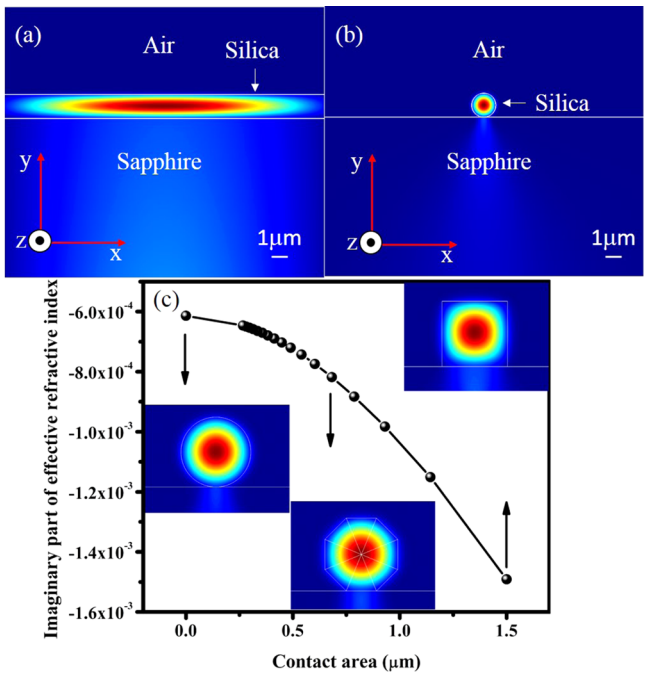

Figure 1. Quasi-guiding modes on a higher index substrate. (a) Slab silica waveguide on sapphire. (b) Silica microfiber on sapphire. Here the waveguide is 600 nm. The height and diameter of the slab and circle are both 1500 nm. (c) Dependence of Im(n_{eff}) on the contact area of the microfiber with a fixed cross-section area.

where a slab waveguide with a 1500 nm thickness is placed on a sapphire substrate. The refractive indices of sapphire and silica are 1.7676 and 1.473, respectively. While light can be weakly confined within the waveguide, the effective refractive index is around 1.4609−0.0015i for the mode at 600 nm. The large imaginary part of the effective refractive index (Im(n_{eff})) corresponds to huge radiation loss. As illustrated in Figure 1a, the numerical results showed that more than 45% of the energy was distributed in the substrate, consistent with the theoretical model well.

Once the cross-section geometry was changed from slab to circle, the light propagation behaviors were totally different. One result is plotted in Figure 1b. The refractive indices are the same as those in Figure 1a, and the diameter of the circle is also 1500 nm. We can see that the mode is mainly confined within the circular region even though its refractive index is much lower than the substrate. The effective refractive index is changed to 1.4453−0.0009i for the mode at 600 nm. In conventional waveguides, a smaller effective refractive index (n_{eff}) means weaker light confinements. Here the loss of a circular waveguide is actually lower than the slab with larger n_{eff}. The percentage of energy in the substrate is only as small as 31.9%, much smaller than the leakage of the slab waveguide. The reduction of light leakage is mainly caused by a smaller contact area between the waveguide and substrate, where the total internal reflection is broken. To characterize the influence of the contact area on light leakage, we conduct a systematic investigation with different contact areas. Here the circle is replaced with a regular polygon, and the total area is fixed at 1500 nm × 1500 nm. Then the contact area can be characterized as the contact length between the microfiber and substrate in cross-section. The calculated results are shown in Figure 1c. It is clear to see that the leakage (imaginary part of effective refractive index) decreases with the reduction of contact area, consistent with the particular cases in Figure 1a and b. Considering the relatively high confinement of light in a microfiber, we call this kind of propagation mode a quasi-guiding mode.

To fully understand the losses of quasi-guiding modes, we have calculated the light propagation with full three-dimensional calculations with the FDTD method. The simulated structure is depicted in Figure 2a, where the diameter of the

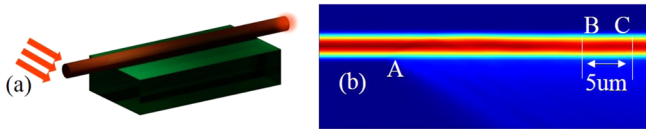

Figure 2. Three-dimensional simulation of a quasi-guiding mode. (a) Schematic picture of a microfiber on a sapphire substrate. (b) Side view of propagation inside a microfiber.

fiber is 2000 nm and the refractive indices are the same as in Figure 1b. The corresponding field distribution in side view is shown in Figure 2b, where several types of radiation losses can be identified. The first loss is the radiation loss from the mode conversion at position A. When the fiber is positioned in air and on a sapphire substrate, their propagation modes are quite different even though both of them are close to fundamental modes. According to the overlap integration, the mode conversion efficiency is very low.[20] The second loss is the propagation loss due to the breaking of total internal reflection. By calculating the transmission between points B and C in Figure 3b, the propagation loss is around 0.03 dB/μm. While the propagation loss is much higher than conventional micro- and nanofibers, it is enough to support a short distance of side−side on-chip direct coupling. Moreover, the propagation loss can be further optimized, as shown below.

Since substrate-induced leaky energy originates from the refractive leakage, we then focused our attention on the influence of the radius of the microfiber and the refractive index of the substrate. Here the transmitted light wavelength and refractive index of the fiber were fixed. All the results are shown

DOI: 10.1021/acsphotonics.5b00176
ACS Photonics 2015, 2, 1278−1283

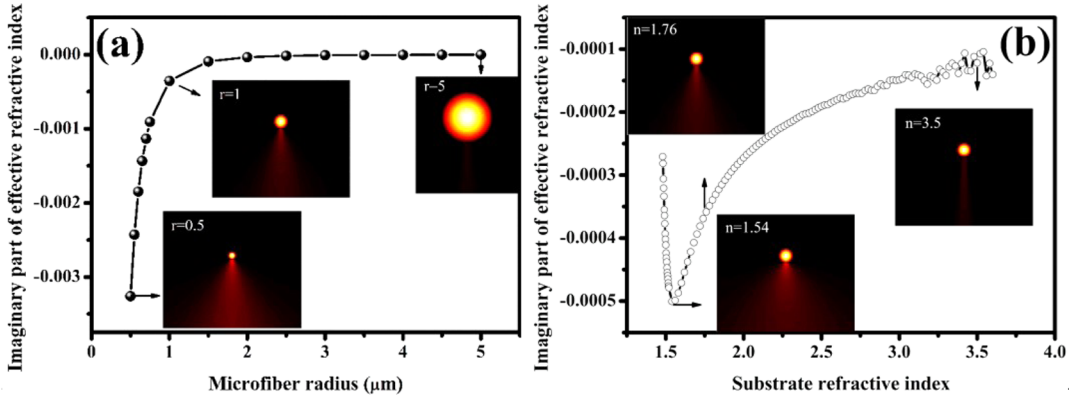

Figure 3. The dependence of Im(n_{eff}) on the radius of a microfiber (a) and refractive index of a substrate (b). The refractive indices of silica and sapphire in (a) are the same as in Figure 1. The radius and refractive index of the silica microfiber in (b) are r = 1000 nm and n = 1.473, respectively. The insets are the cross-sectional field distributions at different conditions marked by the arrows.

in Figure 3. As the nanofiber radius increases, the imaginary part of the effective refractive index increases simultaneously. When the nanofiber radius is larger than 4 μm, the Im(n_{eff}) approaches zero quickly and the energy percent inside the substrate is less than 1%. The smaller Im(n_{eff}) can be easily understood. The modes in Figure 3a are all fundamental modes, whose incident angles increase with an increase of the radius. Following the Fresnel equation, the increased incident angle gives a higher reflectance. Although the total internal reflection at the fiber−substrate interface is broken, the reflectance at large incident angles is also very close to 100%. In this sense, the total loss is decreased at larger radius. A direct comparison of leakage at different r is plotted in the insets of Figure 3a. The leakage at smaller r is quite dramatic and becomes negligible when r is increased to 5 μm.

Figure 3b shows the dependence of Im(n_{eff}) on the refractive index of a substrate. In contrast to the intuitive understanding that more energy will leak into the substrate with higher refractive index, our calculation shows that Im(n_{eff}) decreases first and finally approaches 0 at large refractive index. The leaky loss, in this case, originates from the mode coupling between the waveguide and substrate, which depends on the density of states in the substrate and the corresponding leakage strength, respectively.[19,21,22] Within the range of refractive indices under consideration, the density of states in a substrate is proportional to the substrate refractive index. Meanwhile, the leakage strength is inversely proportional to it. Therefore, the trade-off between the density of states and leakage strength would result in a maximum loss (minimum Im(n_{eff})).

Following the above results, we know that light can be guided within a microfiber even though it was placed onto a higher index substrate. More importantly, the propagation efficiency can be improved when the substrate has a much higher refractive index. This can also be directly observed from the cross-sectional field distributions. As shown in the insets of Figure 3b, less field leaks from the microfiber at a larger refractive index of the substrate. This thus ensures that a microfiber can be positioned onto many types of substrates (see GaN, sapphire for the UV to visible light range, and GaAs, Si for the infrared range) to improve the stability and extends the applications in bridging nanophotonics and traditional optics.

EXPERIMENTAL RESULTS

On the basis of the above descriptions, we then fabricated the microfibers to experimentally test the light propagation on a high refractive index substrate. We first fabricated a silica microfiber with the typical flame-assisted fiber drawing technique and placed it onto a RZJ-304 positive photoresist film that was spin-coated on a standard glass slide substrate. The microscope image of the fabricated microfiber is shown in Figure 4a. The diameter of the microfiber is around 3.2 μm, and

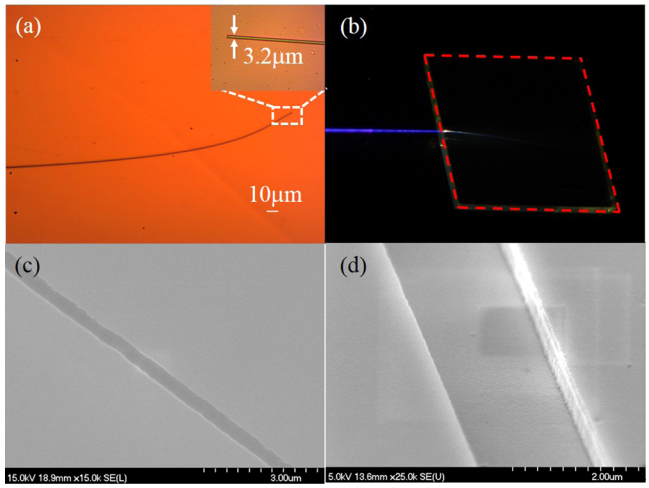

Figure 4. Light propagation in a silica microfiber on an RZJ-304 photoresist substrate. (a) Microscope image of the microfiber. The inset shows the diameter is around 3.2 μm. (b) Propagation of a 365 nm femtosecond laser in a microfiber on an RZJ-304 photoresist. (c and d) SEM pictures of a slot waveguide fabricated by taking advantage of the leaky energy in the substrate.

it is quite uniform within a long distance. Because the microfiber was drawn from a typical single-mode fiber, the untapered end is a conventional single-mode fiber. Thus, a Ti:sapphire laser at 365 nm can be coupled to the fiber through a 20× objective lens. Figure 4b shows the image of light propagation within the microfiber. While different kinds of leakages can be observed, the uniformly decreasing scattered light from the microfiber clearly demonstrates that light can propagate a long distance within the silica microfiber even though it is placed onto a higher index substrate.

In addition to the light propagation within a microfiber, its leakages inside the substrate also keep a narrow beam within a few wavelengths from the fiber−substrate interface (see the insets in Figure 3). In this sense, the microfibers can be used as

DOI: 10.1021/acsphotonics.5b00176
ACS Photonics 2015, 2, 1278−1283

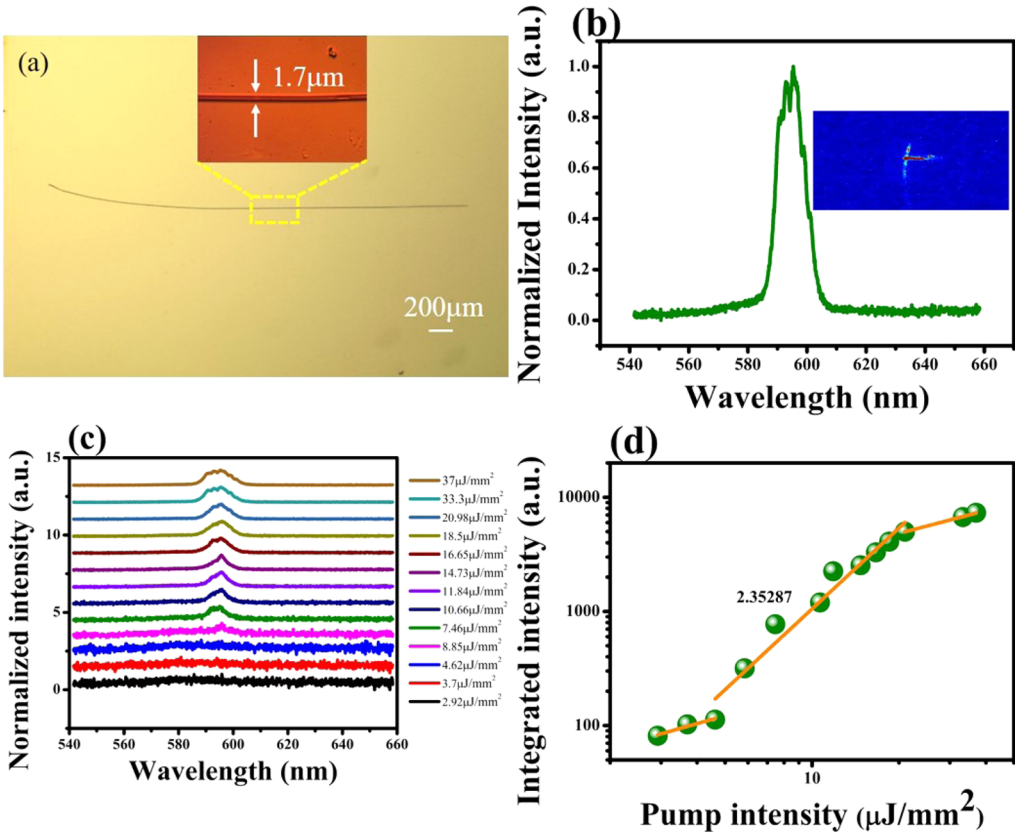

Figure 5. Light amplification in a PMMA microfiber on a sapphire substrate. (a) Microscope image of a dye-doped PMMA microfiber. The diameter of the fiber is around 1.7 μm. (b) Emission spectrum of a PMMA microfiber. Here the pump power is 37 μJ/mm^2. The inset shows the image taken with a conventional camera. (c) Emission spectra from a microfiber under different pumping conditions. (d) Log-scale input−output curves.

a platform to achieve mask-free photolithography. Here we fabricate a slot with this technique to further confirm the light propagation in the microfiber and demonstrate a possible application. The diameter of the silica microfiber is 2.6 μm, which is similar to that in Figure 4a and thus can ensure the long-distance light propagation. Figure 4c exhibits a scanning electron microscope (SEM) picture of a fabricated slot. The width of the slot is as small as 406 nm, which is far smaller than the diameter of the fiber and also much better than the resolution of standard photolithography. Interestingly, the width of the slot is quite uniform not only in the SEM image (>10 μm in length) but also several hundred micrometers under a microscope. Figure 4d shows a tilt-view SEM image of another slot waveguide. More than the uniformity in width, here we can also see that the sidewalls are quite straight in the vertical direction. It is worth noting that both SEM pictures show some roughness. This is mainly induced by the tiny vibration of the microfiber during the long exposure time (a few to 10 min) and can be eliminated by optimizing the exposure conditions. Considering the easy fabrication of the microfiber, this technique can enable a cost-effective fabrication of nanostructures such as straight or curved waveguides.

More than the observation of light propagation, we have also tested the possible light amplification and laser behaviors in microfibers. This information is also important for developing efficient couplers or active integrated elements. Here the microfiber was fabricated by direct drawing from a rhodamine B (RhB)-doped poly(methyl methacrylate) (PMMA) solution. The PMMA solution was synthesized by dissolving 1 g of PMMA and 0.01 g of RhB into a chloroform solvent. The diameter of the as-drawn microfiber was controlled by the drawing speed and the concentration of the PMMA solution. The fabricated PMMA microfiber (n = 1.49) was placed onto a sapphire substrate (n = 1.7676) and pumped with a frequency-doubled Nd:YAG laser (pulse width 6 ns, 10 Hz, 532 nm). The pumping laser was focused by a cylindrical lens (f = 25 cm) and formed a laser stripe along the axis of the microfiber.[21] The width of the laser stripe was controlled by a slit. The outputs from the microfiber were collected by a lens and coupled to a CCD-based spectrometer.

Figure 5b shows an example of an emission spectrum from a microfiber. The pump density is 37 μJ/mm^2. We can see that the line width is only around 10 nm, which is much smaller than the typical photoluminescence of RhB dye. Figure 5c shows the spectrum as a function of pump power. With the increase of pump density, we can clearly see a transition from a broad photoluminescence peak to a narrow peak when the pump density is larger than 5.85 μJ/mm^2. The corresponding integration of the output has been summarized in Figure 5d in log scale. A clear threshold behavior can be observed from the "S" shape.[22] The threshold is around 5 μJ/mm^2. The slope increases from ∼1 to 2.35 when the pumping power passes the threshold and finally changes back to ∼1. This "S" shape demonstrates the existence of an amplified stimulated emission (ASE) well.

The threshold clearly demonstrates the amplification inside the microfiber. As only the propagating waves along the microfiber can be amplified, Figure 5 also gives an additional proof for the existence of quasi-guiding modes when the microfiber is placed onto a higher index substrate. The inset in

DOI: 10.1021/acsphotonics.5b00176
ACS Photonics 2015, 2, 1278−1283

Figure 5b is the image of a nanowire under optical pumping. Consistent with the amplification, we can directly see that most of the light is confined along the nanowire, where the intensity is much higher than the others. In the inset of Figure 5b, slight emissions from the substrate can also be observed at the edge of the substrate (see the dashed line). This kind of emission is mainly caused by the leakage from the microfiber, consistent with the numerical calculations in Figure 2. Moreover, as the leakages are no longer confined by the microfiber, a large divergent beam instead of directional output at the boundary of the substrate was recorded in the images.

On the basis of the light amplification inside the polymer microfiber, we then studied the corresponding laser actions inside it. Due to the absence of optical feedback, the microfiber itself does not support laser action. We then tailor the microfiber into a knot resonator under a microscope (see inset in Figure 6a). Within the microknot, light can be well trapped

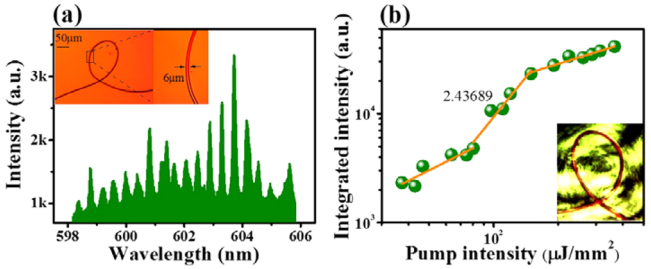

Figure 6. Lasers in the PMMA microfiber knot cavity on a sapphire substrate. (a) Laser spectrum from the microfiber knot cavity. The inset is the microscope image of a dye-doped PMMA microfiber. The diameter of the fiber is increased 6 μm. (b) Threshold behaviors of lasers. The inset shows an optical image of a microknot under optical excitation.

by total internal reflection and circulates inside it through the coupling at the joint position.[1] In this sense, whispering gallery modes can be formed and lasing actions can be generated under optical excitation.

Figure 6a shows the emission spectrum from the microknot when it is excited under a microscope (see the inset in Figure 6b). Different from the broad ASE peak in Figure 5, periodically narrow peaks with equal mode spacing can be clearly observed in Figure 6a. The measured mode spacing in Figure 6a is around 0.414 nm, which is a little bit smaller than the estimated free spectral range of whispering gallery modes ($\Delta\lambda = \lambda^2/(n_{\mathrm{eff}}L) \approx 0.456$ nm). This deviation results from the refractive index change of a dye-doped PMMA microfiber under optical excitation[23] and the error of the knot cavity perimeter in the measurement. The line width of the laser peak is about 0.12 nm, which is more than 2 orders of magnitude smaller than the ASE. The dependence of the emission intensity on pumping power has been summarized in Figure 6b. An "S" shape can be clearly observed and gives a laser threshold at around 80 μJ/mm^2.

One key information in Figure 6 is that the lasing action can be formed on a substrate with a higher refractive index. It can immediately bridge two initially unrelated research areas. One is a microtoroid laser pioneered by Armani et al.[24] and has great potential in ultra-low-threshold light sources.[25] The other one is a CMOS-compatible laser, which is a key element of on-chip optical interconnects and currently hindered by the fabrication techniques in III–V materials. Our finding can thus give an alternative approach by utilizing microtoroid lasers on silicon. For a first step, we have numerically calculated the resonances inside it. Our calculation shows that the Q factor of the whispering gallery mode can easily be above 10^6, and it can be increased to 10^7–10^8 after optimizing the parameters. Therefore, it is possible to realize on-chip laser sources with ultra-low-energy consumptions.

CONCLUSION

We have numerically and experimentally studied the possibility of light propagation in a microfiber that is placed on a higher index substrate. In contrast to the intuitive picture, we found that the fundamental modes could be considered as quasi-guiding modes. The propagating loss of quasi-modes can be minimized by changing the size of the microfiber and the refractive index of the substrate, and the loss of silica microfibers on silicon is negligibly small. By utilizing sapphire as a substrate, we have experimentally verified the light propagation and amplification in silica and PMMA microfibers. In a knot cavity constituted by a RhB-doped PMMA microfiber, the lasing actions have also been observed. Our finding is a new propagating status and can significantly help the interconnection between conventional fiber optics and micro- or nanophotonics. In addition, it can also have important impacts on mask-free photolithography and CMOS-compatible on-chip light sources.

AUTHOR INFORMATION

Corresponding Author

*E-mail: qinghai.song@gmail.com.

Notes

The authors declare no competing financial interest.

ACKNOWLEDGMENTS

This work is supported by NSFC11204055, NSFC61222507, NSFC11374078, NCET-11-0809, Shenzhen Peacock plan under the Nos. KQCX2012080709143322 and KQCX20130627094615410, and Shenzhen Fundamental research projects under the Nos. JCYJ20130329155148184, JCYJ20140417172417110, and JCYJ20140417172417096.

REFERENCES

(1) Tong, L. M.; Gattass, R. R.; Ashcom, J. B.; He, S. L.; Lou, J. Y.; Shen, M. Y.; Maxwell, I.; Mazur, E. Subwavelength-diameter silica wire for low-loss optical wave-guiding. *Nature* **2003**, *426*, 816–819.

(2) Guo, X.; Qiu, M.; Bao, J. M.; Wiley, B. J.; Yang, Q.; Zhang, X. N.; Ma, Y. G.; Yu, H. K.; Tong, L. M. Direct Coupling of Plasmonic and Photonic Nanowires for Hybrid Nanophotonic Components and Circuits. *Nano Lett.* **2009**, *9*, 4515–4519.

(3) Law, M.; Sirbuly, D. J.; Johnson, J. C.; Goldberger, J.; Saykally, R. J.; Yang, P. D. Nanoribbon Waveguides for Subwavelength Photonics Integration. *Science* **2004**, *35*, 1269–1273.

(4) Cassidy, D. T.; Johnson, D. C.; Hill, K. O. Wavelength-dependent Transmission of Monomode Optical Fiber Tapers. *Appl. Opt.* **1985**, *24*, 945–950.

(5) McCallion, K.; Johnstone, W.; Fawcett, G. Tunable in-line Fiber-optic Bandpass Filter. *Opt. Lett.* **1994**, *19*, 542–544.

(6) Ta, V. D.; Chen, R.; Ma, L.; Ying, Y. J.; Sun, H. D. Whispering Gallery Mode Microlasers and Refractive Index Sensing Based On Single Polymer Fiber. *Laser Photonics Rev.* **2013**, *7*, 133–139.

(7) Lou, J. Y.; Wang, Y. P.; Tong, L. M. Microfiber Optical Sensors: A Review. *Sensors* **2014**, *14*, 5823–5844.

(8) Yu, X. C.; Li, B. B.; Wang, P.; Tong, L. M.; Jiang, Z. F.; Li, Y.; Gong, Q. H.; Xiao, Y. F. Single Nanoparticle Detection and Sizing

DOI: 10.1021/acsphotonics.5b00176
ACS Photonics 2015, 2, 1278–1283

Using a Nanofiber Pair in an Aqueous Environment. *Adv. Mater.* **2014**, *26*, 7462−7467.
(9) Jiang, X. S.; Song, Q. H.; Xu, L.; Fu, J.; Tong, L. M. Microfiber knot dye laser based on the evanescent-wave-coupled gain. *Appl. Phys. Lett.* **2007**, *90*, 233501.
(10) Xiao, Y.; Meng, C.; Wang, P.; Ye, Y.; Yu, H. K.; Wang, S. S.; Gu, F. X.; Dai, L.; Tong, L. M. Single-Nanowire Single-Mode Laser. *Nano Lett.* **2011**, *11*, 1122−1126.
(11) Song, Q. H.; Liu, L. Y.; Xu, L. Lasing action in dye doped polymer nanofiber knot resonator. *J. Lightwave Technol.* **2009**, *27*, 4374−4376.
(12) Cai, M.; Painter, O.; Vahala, K. J. Observation of critical coupling in a fiber taper to a silica-microsphere whispering-gallery mode system. *Phys. Rev. Lett.* **2000**, *85*, 74−77.
(13) Huang, K. J.; Yang, S. Y.; Tong, L. M. Modeling of Evanescent coupling between two parallel optical nanowires. *Appl. Opt.* **2007**, *46*, 1429−1434.
(14) Coillet, A.; et al. Near-field characterization of glass microfibers on a low-index substrate. *Appl. Phys. B: Lasers Opt.* **2010**, *101*, 291−295.
(15) Pyo, J.; et al. Light propagation in conjugated polymer nanowires decoupled from a substrate. *Nanoscale* **2014**, *6*, 5620−5623.
(16) Tong, L. M.; Lou, J. Y.; Gattass, R. R.; He, S. L.; Chen, X. W.; Liu; Mazur, E. Assembly of Silica Nanowires on Silica Aerogels for Microphotonic Devices. *Nano Lett.* **2005**, *5*, 259−62.
(17) Chaudhari, C.; Liao, M. S.; Suzuki, T.; Ohishi, Y. Chalcogenide Core Tellurite Cladding Composite Microstructured Fiber for Nonlinear Applications. *J. Lightwave Technol.* **2012**, *30*, 2069−2076.
(18) Xu, Q.; Almeida, V. R.; Panepucci, R. R.; Lipson, M. Experimental demonstration of guiding and confining light in nanometer-size low-refractive-index material. *Opt. Lett.* **2004**, *29*, 1626−1628.
(19) Zou, C. L.; Cui, J. M.; Sun, F. W.; Xiong, X.; Zou, X. B.; Han, Z. F.; Guo, G. C. Guiding light through optical bound states in the continuum. *Laser Photonics Rev.* **2015**, *9*, 114−119.
(20) Gu, Z. Y.; Liu, S.; Sun, S.; Wang, K. Y.; Lyu, Q.; Xiao, S. M.; Song, Q. H. Photon hopping and nanowire based hybrid plasmonic waveguide and ring-resonator. *Sci. Rep.* **2015**, *5*, 9171.
(21) Zou, C. L.; Sun, F. W.; Xiao, Y. F.; Dong, C. H.; Chen, X. D.; Cui, J. M.; Gong, Q.; Han, Z. F.; Guo, G. C. Plasmon modes of silver nanowire on a silica substrate. *Appl. Phys. Lett.* **2010**, *97*, 183102.
(22) Zou, C. L.; Chen, X. D.; Xiong, X.; Sun, F. W.; Zou, X. B.; Han, Z. F.; Guo, G. C. Photonic simulation of system-environment interaction: Non-Markovian processes and dynamical decoupling. *Phys. Rev. A: At., Mol., Opt. Phys.* **2013**, *88*, 063806.
(23) Lebental, M.; Djellali, N.; Arnaud, C.; Lauret, J. S.; Zyss, J.; Dubertrand, R.; Schmit, C.; Bogomolny, E. Inferring periodic orbits from spectra of simply shaped microlasers. *Phys. Rev. A: At., Mol., Opt. Phys.* **2007**, *76*, 023830.
(24) Armani, D. K.; Kippenberg, T. J.; Spillane, S. M.; Vahala, K. J. Ultra-high-Q toroid microcavity on a chip. *Nature* **2003**, *421*, 925−928.
(25) Jiang, X. F.; Xiao, Y. F.; Zou, C. L.; He, L. N.; Dong, C. H.; Li, B. B.; Li, Y.; Sun, F. W.; Yang, L.; Gong, Q. H. Highly Unidirectional Emission and Ultralow-Threshold Lasing from On-Chip Ultrahigh-Q Microcavities. *Adv. Mater.* **2012**, *24*, OP260−OP264.

DOI: 10.1021/acsphotonics.5b00176
ACS Photonics 2015, 2, 1278−1283